Aligning the Demonstration Model of CHEOPS

M. Bergomi[*a], F. Biondi[a], L. Marafatto[a], M. Dima[a], D. Greggio[a,b], J. Farinato[a], D. Magrin[a], R. Ragazzoni[a], V. Viotto[a], M. Gullieuszik[a], G. Farisato[a], L. Lessio[a], E. Portaluri[a], M. Munari[c], I. Pagano[c], M. Marinai[d], A. Novi[d], C. Pompei[d], D. Piazza[e], T. Beck[e], V. Cessa[e], W. Benz[e]

[a] INAF - Osservatorio Astronomico di Padova, Vicolo dell'Osservatorio 5, 35122 Padova, Italy
[b] Dipartimento di Fisica ed Astronomia - Università degli Studi di Padova, Vicolo dell'Osservatorio 3, 35122 -Padova, Italy
[c] INAF - Osservatorio Astrofisico di Catania, Via S.Sofia 78, 95123 Catania, Italy
[d] Leonardo Spa - Eo Payloads/ Propulsion Techn. & Assembly, Via A. Einstein 35, 50013- Campi Bisenzio (Firenze), Italy
[e] Physikalisches Institut - Universität Bern, Sidlerstrasse 5, 3012 Bern, Switzerland

ABSTRACT

CHEOPS (CHaracterizing ExOPlanets Satellite) is an ESA Small Mission, planned to be launched in mid-2018 and whose main goal is the photometric precise characterization of radii of exoplanets orbiting bright stars (V<12) already known to host planets.
Given the fast-track nature of this mission, we developed a non-flying Demonstration Model, whose optics are flight representative and whose mechanics provides the same interfaces of the flight model, but is not thermally representative.
In this paper, we describe CHEOPS Demonstration Model handling, integration, tests, alignment and characterization, emphasizing the verification of the uncertainties in the optical quality measurements introduced by the starlight simulator and the way the alignment and optical surfaces are measured.

Keywords: CHEOPS, exoplanets, transits, ESA, Small mission, telescope, AIV, prototyping

1. INTRODUCTION

CHEOPS (CHaracterizing ExOPlantes Satellite)[1][2] is a joint ESA-Switzerland Small Mission, adopted in 2014 and planned to be launched in mid-2018. It will be sent into a low Earth (650-800 km) sun-synchronous orbit, with the main goal to perform, through the transit method, the precise characterization of radii of exoplanets orbiting bright stars (V<12) already known to host planets.
One of the main criticality in the development of such a system is the need to reach an extremely high photometric stability, driving its opto-mechanical design mainly in two fields: extreme structure stability and very high degree of straylight suppression. Details on the techniques developed to cope with this issue, along with the project status, can be found in [3], [4] and [5].
As for every space mission, the development of intermediate models is extremely important in order to decrease all possible risks. In particular, being CHEOPS a fast-track mission, it is of paramount importance to demonstrate the feasibility or criticalities of the AIV procedures, as well as the development of adequate Ground Support Equipment (GSE), ahead of their implementation on the Proto-Flight Model (PFM) by the Italian Prime contractor LEONARDO Spa (formerly SELEX ES), supervised by INAF.
For this reason, in collaboration with the University of Bern and LEONARDO, a Demonstration Model (DM) of CHEOPS telescope was developed. It consists in a non-flying CHEOPS model, whose mechanics is fully representative concerning interfaces but not thermally equivalent, and whose optics exhibits optical quality and handling capabilities very close to the flight model, allowing to test procedures for handling, integration, alignment and characterization.

[*] maria.bergomi@oapd.inaf.it

Space Telescopes and Instrumentation 2016: Optical, Infrared, and Millimeter Wave, edited by Howard A. MacEwen, Giovanni G. Fazio, Makenzie Lystrup, Proc. of SPIE Vol. 9904, 990439 · © 2016 SPIE · CCC code: 0277-786X/16/$18 · doi: 10.1117/12.2232136

In this paper, we describe the main steps and results of the work performed at the laboratories of INAF Padova, where the CHEOPS DM was assembled, aligned and tested in ambient temperature, with emphasis on the verification of the uncertainties in the optical quality measurements introduced by the starlight simulator and the way the alignment and optical surfaces are measured.

2. CHEOPS TELESCOPE DEMONSTRATION MODEL

Different models were foreseen to thoroughly test the system, even in a schedule as tight as CHEOPS one: a Structural Thermal Model, an Engineering Qualification Model, a DM, and, finally, the PFM. The DM model has been realized only for the telescope, the so-called TEL subsystem. It is composed by two optical systems and their mechanical structure: a compact on-axis F/5 Ritchey-Chrétien two mirrors centered telescope, with an aperture of 320 mm and a Back-End Optics (BEO), reshaping a defocused PSF on the detector [6]. The latter is due to the choice of spreading the PSF over a quite large amount of pixels to average for single-pixels anomalies (see also [7]). This, together with an intermediate pupil mask for the straylight rejection and a baffle with vanes preceding the telescope, are the solutions foreseen to obtain very high photometry stability. The main parameters of the final optical configuration are collected in Table 1.

Table 1. Main parameters of the optical configuration.

Spectral range	400 – 1100 nm
Entrance pupil diameter	320 mm
Central obstruction diameter	68 mm
Working F/#	8.38 @ 750 nm
Field of View (diameter)	0.32 degrees
Effective focal length	2681 mm @ 750 nm
Pixel size	13 micron
Plate scale	1 arcsec/pixel

In Figure 1 it is shown a CAD view of the TEL DM structure, made by the assembly of:

- an opto-mechanical Tube, consisting of a mechanical structure mounting the hyperbolic primary (M1) and secondary (M2) mirrors
- an Optical Bench Assembly (OBA)
- the BEO, consisting of a mechanical part mounting a set of small optics, a doublet (D1), collimating the light coming from the tube, a pupil mask, a folding mirror (M3) to direct the light toward the detector and a second doublet (D2) to focus the PSF onto the detector.

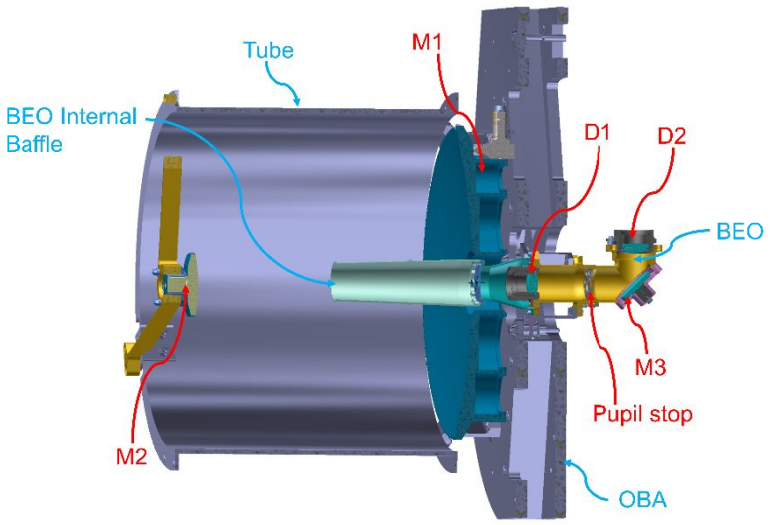

Figure 1. CAD section view of TEL DM. Main components are indicated (blue mechanics, red optics).

The DM mechanical structure has been realized by University of Bern in anodized aluminum rather than in carbon fiber as the final one. The DM optical groups (optics and their mechanics) have been manufactured in flight materials by LEONARDO and subcontractors, differing from flight optics for not being radiation-hardened, the coatings and the level of light-weighting of M1. Both DM optics and mechanics are shown in Figure 2. Glue acts as interface between mirror groups and mechanics and it is injected after alignment is completed.

Figure 2. On top are DM mechanics components, while on the bottom DM mirrors held by their alignment tools (on M1G a partial light-weighting can be observed).

3. REFERENCES AND REQUIREMENTS

The main requirement on the TEL alignment is that the optical axis shall be aligned with respect to (wrt hereafter) the OBA reference frame (OBA side facing M1) with a precision of ± 500 μm in centering and ± 400 μrad in tilt. The reference for centering is given by the pins were M1/tube supports are connected.

The foreseen alignment procedure strategy, whose preliminary version was described in [6], consists in a two-step alignment: firstly, the Tube (M1-M2) is aligned with respect to the OBA; afterwards BEO is aligned with respect to the Tube (currently on-going activity).

In this view, the overall requirement has been split between different components: on M1 an alignment of ± 100 μm in centering and focus and ± 300 μrad in tilt is required. Furthermore, to guarantee the needed optical quality, M2 has to be aligned with respect to M1 with a precision of ± 5 μm in centering and focus and ± 26 μm in tilt. Concerning BEO, requirements on internal alignment are mainly translated into mechanical tolerances we will not detail, while overall BEO wrt to Tube tolerances are translated into ± 10 μm in focus, ± 30 μm in centering and ± 600 μrad in tilt. The only optical element inside BEO with autonomous adjustment capability is D2 in focus direction (its alignment accuracy should be ± 5 μm from Focal Plane).

4. ALIGNMENT PROCEDURE & GSES

In order to fulfill the previously given requirements, the following integration and alignment strategy, along with realization of specifics Optical and Mechanical GSEs (see Figure 3 and Figure 4), were determined and are hereafter summarized:

1. **Alignment reference definition**
   the bearing mechanical axis is aligned (center and tilt) to the mechanical references on the OBA, therefore materializing the optical axis of the system.

MGSEs:

- **handling**, used to support TEL DM into a vertical configuration;
- a **bearing** (wobble ~60 μrad), equipped with a small optical bench and a centering and tilt adjustment system, located on the handling base-plate;
- a "**ring**", connected to the OBA centering reference pins (0.02 mm precision wrt nominal mechanical reference);
- a **column**, equipped with **dial gauges** (2 μm accuracy) fixed onto the bearing, allows to touch the inner part of the ring and its bottom side, and, minimizing the value measured during a 360° rotation, to align the bearing to the reference plane.

2. M1 alignment to the OBA reference plane

M1 MGSE: a manipulator (visible in Figure 2 bottom left), equipped with three flexible blades supporting M1 (through specific channels present on each M1 bush). It is provided with two micrometers (0.1 μm sensitivity) for decenter and three micrometers (1 μm sensitivity) for tilt, corresponding to 0.75". The tilt micrometers can provide also focus adjustment if shifted simultaneously by the same amount. The manipulator is installed onto a cart (orange in Figure 3), to be inserted under the OBA.

- M1 centering alignment is obtained mechanically aligning M1 to the bearing mechanical axis, with the same concept used for the reference alignment, minimizing the value measured by a dial gauge touching the inner hole of M1during a 360° rotation.
  MGSEs: same as phase 1 (no ring).
- M1 tilt alignment is obtained minimizing a spot trajectory produced during a 360° rotation by a laser integral to the bearing.
  GSE: a laser shining toward M1 and a camera recording the spot trajectory during a bearing rotation (both are integral to the bearing).
- M1 focus is adjusted mechanically to nominal values.

The previous three steps are of course iterated until reaching values inside requirements.

3. M1 gluing

After the alignment is obtained and its stability verified, M1 can be glued to its support injecting bi-component glue Hysol 9493 and letting it cure for approximately a week. Afterwards the manipulator can be removed.

4. Preliminary operations for M2 alignment

The requirement on M2 specified in Section 3 was translated into the minimization of tilt, power and coma Zernike coefficients below 0.05 λ in an interferometric double-pass alignment.

M2 OGSE: Zygo FlashPhase GPI interferometer (λ=632.8 nm) and a 330 mm collimated beam (COLL, obtained aligning an F/1.5 spherical element and a 330 mm Off-Axis Parabola, OAP).

- M1 optical axis materialization, through a flat mirror aligned to the bearing with an autocollimator.
  GSEs: a 100 mm diameter flat mirror (FM1) installed over the OBA, facing down, equipped with tip-tilt adjustments; an autocollimator; the bearing assembly.
- TEL focal plane materialization, through a spherical gauge aligned to the bearing with a setup similar to the one used for M1 tilt alignment.
  GSEs: a 25 mm diameter spherical mirror with radius of curvature 100 mm (SM1), equipped with x-y-z stages allowing to center it wrt M1 (minimizing a spot trajectory produced during a 360° rotation by a laser integral to the bearing) and adjust it in focus to the nominal position.
- Collimated beam alignment to the optical axis, thanks to a large flat mirror 45°-oriented located just over the bearing (Figure 3, left).
  GSE: a 480 mm diameter λ/57 rms flat mirror (FM2), equipped with tip-tilt adjustment.

5. M2 alignment to M1

M2 is aligned wrt M1 in tilt, focus and center minimizing the Tilt, Power and Coma Zernike coefficients retrieved by the interferometer M2.

M2 MGSE: M1 manipulator can be slightly modified, inserting a spider-shaped support to hold M2 (visible in Figure 2, bottom right).

6. M2 gluing

After the alignment is obtained and stability verified, M2 can be glued to its support injecting bi-component glue Hysol 9493, while monitoring the interferometric pattern and letting it cure for approximately a week. Afterwards the manipulator is removed.

7. Align BEO with respect to the Tube (M1-M2)

A strategy similar to M2 alignment is foreseen, with a spherical gauge mechanically positioned by means of a Coordinate Measuring Machine onto the focal plane and the BEO adjusted in tilt, focus, center and rotation, minimizing interferometric Zernike coefficients.

GSEs: spherical gauge located on the focal plane, BEO manipulator with centering, focus and rotation capabilities. Shims are used to adjust BEO tilt.

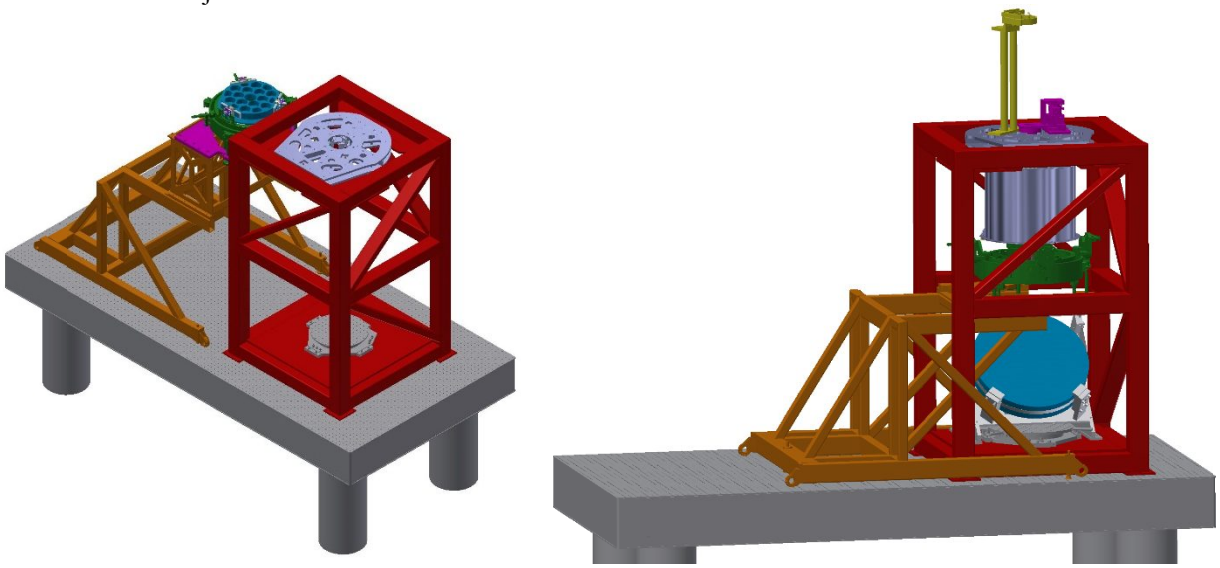

Figure 3. CAD views of the optical bench for CHEOPS DM AIV. The handling is the red structure holding the OBA in a first stage and then the full TEL; the manipulator cart (orange) can be partially modified to accommodate manipulator (green) for M1 and M2 alignment; the bearing assembly (gray) can be seen on the handling base-plate. *Left*: setup for bearing alignment and ready for M1 alignment. *Right*: setup for M2 alignment, an incoming 330-mm collimated beam is directed toward the TEL by a large flat mirror 45°-oriented. On top of the OBA are installed FM1 (yellow) and SM1 (pink), the latter installed onto a kinematic repositionable plate.

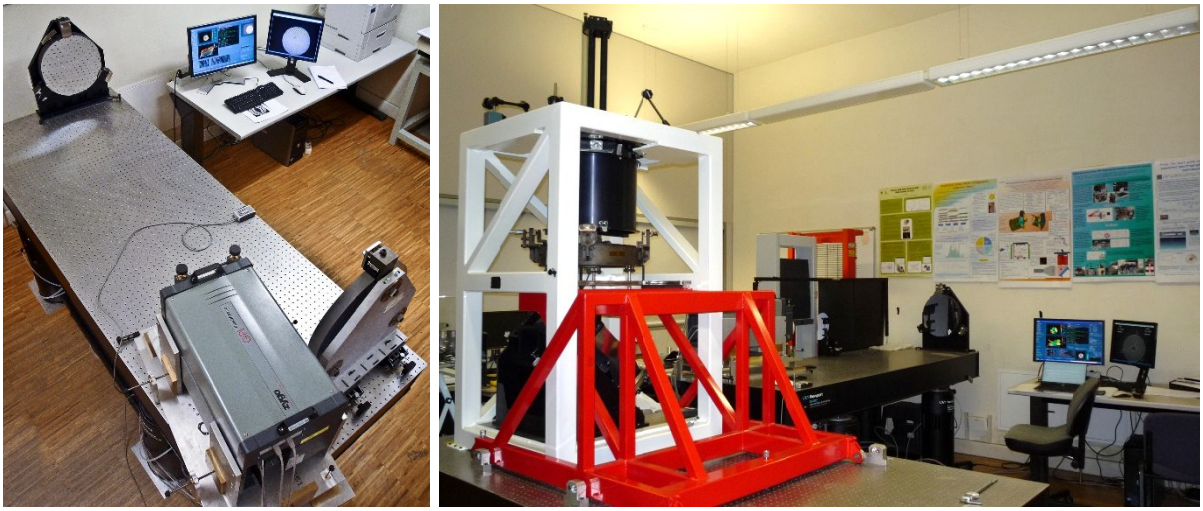

Figure 4. Actual laboratory setup at INAF-Padova for the DM AIV. *Left*: the setup to obtain the 330 mm collimated beam (with a reference flat mirror used for its alignment). *Right:* overall setup during M2 alignment phase.

5. ALIGNMENT RESULTS

The DM TEL AIV activity comprises two tube alignments campaigns. During the first one, a few issues were identified and addressed, but a poor quality in the tube/M1 support surfaces coupling translated in a very large astigmatism (estimated in more than 5 λ Peak to Valley, PtV) that would not allow to fully test the AIV procedure. The alignment was repeated after a very precise machining of the two surfaces, when a planarity lower than 10 μm was obtained, and implementing some of the lessons learned from the first run.
The main results of the second campaign will hereafter be summarized, focusing on the setup optical quality characterization and analysis of M1-M2 alignment, including its dependence on temperature and M2 rotation. We remind that BEO integration and alignment are currently on going.

5.1 M1 alignment

Following the procedure and the tools described in Section 4 (bullets 1 and 2), M1 was aligned in tilt, center and focus with respect to the reference plane defined on the OBA. Leaving aside the technicalities of the several steps leading to this alignment, Table 2 summarizes the main effects contributing to M1 alignment budget, summed in quadrature. An unavoidable contribute is given by the bearing wobble and runout, affecting also its alignment wrt OBA and therefore the reference for M1 alignment. In addition to these values, we have to include the machining precision of M1 hole with respect to its optical axis and to consider the effect of M1 decenter onto M1 tilt. The latter, in fact, while adjusted, tries to compensate the decenter, leading to a tilt misalignment. To be conservative we can sum linearly this contribution to the previous one, obtaining a total M1 tilt of approximately 258.7 (± 129.3) μrad - corresponding to approximately 53.6 (± 26.8)"- still below the 400 μrad of tolerance.

Table 2. Error contributions to M1 alignment wrt OBA.

Contribute	**Decenter (μm)**	**Tilt (μrad)**
Bearing wobble	35	60
Bearing run-out	15	--
Residual tilt	--	73
Residual decenter	32	--
Measurement accuracy (dial gauge sensitivity + setup stability)	4	--
Bearing misalignment	40.1	62.5
M1 optical axis wrt central hole	50	--
Total	81.2	113.3
Effect of maximum decenter on tilt.	--	145.4
Overall total	**81.2 (± 40.6)**	**258.7 (± 129.3)**

5.2 Setup optical elements and DM mirrors characterization

Before proceeding to M2 alignment through double-pass interferometric measurements, we characterized our starlight simulator, along with the other setup mirrors, in order to minimize their impact on the overall alignment result. All measurements are expressed in wavelength (λ=632.8 nm) and the wavefronts (obtained from an average of 100 measurements) are shown in Figure 5.

In order to reduce the aberration on the collimator, its optics were aligned using the double-pass interferometric setup visible in Figure 4, which included also a 400-mm diameter reference flat whose optical quality is λ/10. The Zygo interferometer with its reference sphere was equipped with x-y-tip-tilt-rotation micrometric adjustments, while the OAP had previously be roughly aligned inside its own mount to have the optical axis almost parallel to the optical bench. Looking at the double pass interferograms, the main aberrations were minimized. To further reduce the aberrations produced by stress on the optics, OAP and reference mirror mount holders were properly tuned. The final result is 0.32 PtV, 0.07 rms, and the largest residual aberration is the spherical one, of the order of 0.1 λ.

Afterwards, to determine the effect of FM2, the collimated beam reached the large 45°-oriented mirror and the reference flat mirror was held horizontally on three points above FM2. The overall obtained result is slightly larger wrt the previous one (0.43 PtV, 0.09 rms), with a distinguishable trefoil mainly due to the reference mirror holding.

The other critical optical component to be tested was SM1, the spherical gauge. We tested different mirrors and selected the one with the lower aberrations. The latter was then tested inside its own mount, which was modified until obtaining the very satisfying value of 0.1 PtV, 0.08 rms.

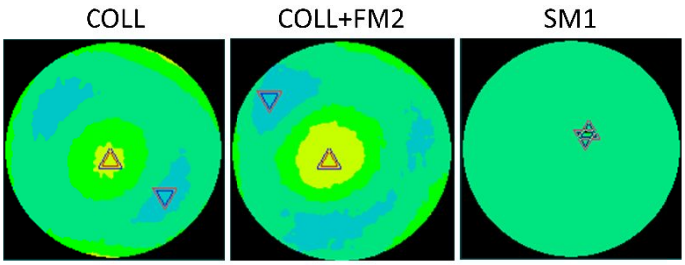

Figure 5. Wavefronts (obtained by the average of 100) of the main optical elements used during M2 alignment, the collimator, the large 45°oriented flat mirror and the spherical gauge.

Furthermore, to have a qualitative and quantitative idea of the aberrations introduced by DM mirrors, their optical quality was reported to us by LEONARDO and the wavefronts are shown in Figure 6. It is important to note that M1 was measured while laying on its rear-side and before the bushes were glued to the mirror.

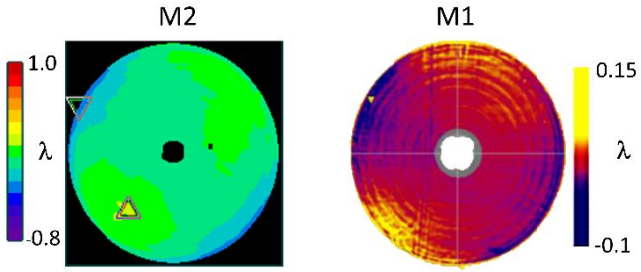

Figure 6. DM M1 and M2 wavefronts, provided by LEONARDO.

5.3 M2 alignment

As first thing, to understand the impact of the tube on the primary mirror aberrations, we performed the alignment with M2 held by its manipulator but without installing the tube (see Figure 7).

In this phase, after M2 alignment was performed, we noticed a dominant astigmatism of the order of 0.7 λ on an overall PtV of 1.8 λ. The analysis to understand its origin identified M1 as the main responsible. In fact, between the first and second alignment, M1 was rotated of 120° and so does the astigmatism. This is clearly visible in the wavefronts Figure 7 (thanks to an imperfection in M1 grinding - noticeable also in Figure 6 - that has been marked by a dashed line).

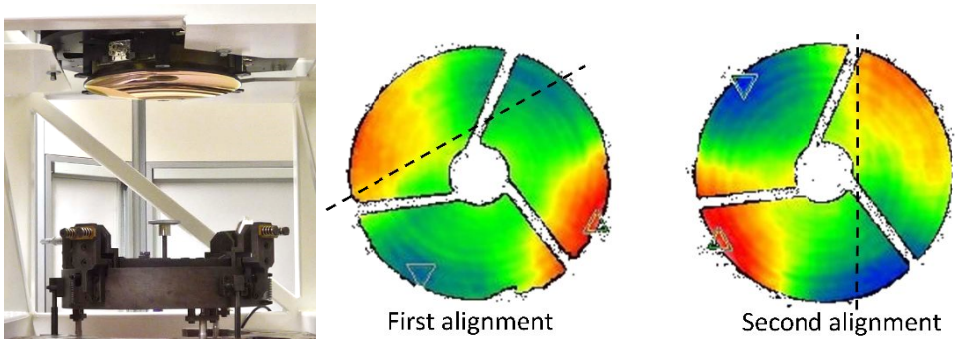

Figure 7. *Left:* M1 glued to OBA and M2 located on manipulator during the first phase of M2 alignment (performed without the tube). *Right:* wavefronts obtained in this configuration during first and second alignment of the tube. M1 was rotated, as clearly visible from an imperfection in M1 itself, marked by a dashed line.

When the tube was installed, variations of the order of 0.2 PtV were observed on the wavefront. The Zernike's coefficients varying the most were the spherical coefficient, which decreased by about 0.05 λ and the trefoil. The latter variation cannot be explicitly determined, even though the order of magnitude is 0.1 λ, since it shows a strong dependence on temperature, which was not monitored during this operation. Given the correspondence of the trefoil direction to the three M1 attachment points, we infer that this effect is mainly due to the mismatch between M1G, made of zerodur and invar, with respect to OBA, realized in aluminum.
Since our laboratory showed a variation in temperature of a few degrees during the AIV phase, we tested the dependence of all the main Zernike coefficients from the temperature. The main dependence is of course the focus term, which could however be adjusted with the manipulator (of course before gluing M2 to the spider). The second most evident is trefoil, which increases at the increase of temperature. The relationships between the main Zernike coefficients and temperature before and after M2 gluing are reported in Figure 8.

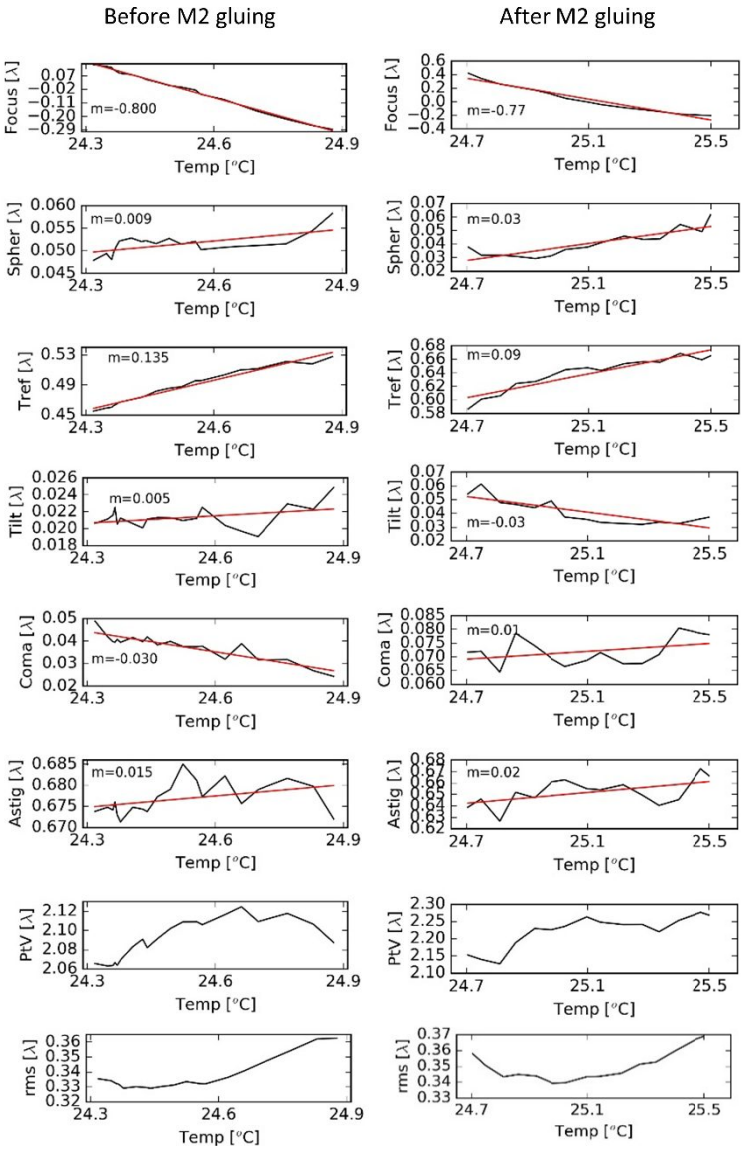

Figure 8. Variation of main Zernike's coefficients with temperature during alignment phase (left) and after M2 gluing is completed (right). Before gluing, tilt, power and coma can be compensated with manipulator, while trefoil is probably dependent on the mismatch between M1G zerodur and invar with respect to OBA aluminum. For tilt, coma, astigmatism and trefoil, we consider the sum in quadrature of the two coefficients.

Another aspect that we investigated was the influence of M2 rotation on astigmatism and trefoil, since, as visible in Figure 6 they are the two dominant aberrations on M2. After each rotation (operation assisted by a goniometer installed on the manipulator), M2 was aligned wrt to M1 and 50 wavefronts were averaged. After correcting the obtained values for temperature modulating all of them at T=24.3°C (with the relationship shown in Figure 8, as expected, a minimum for astigmatism over 180° and a minimum for trefoil over 120° was observed. Given the dominance of the astigmatism aberration, we selected M2 rotation angle corresponding to the minimum of the astigmatism.

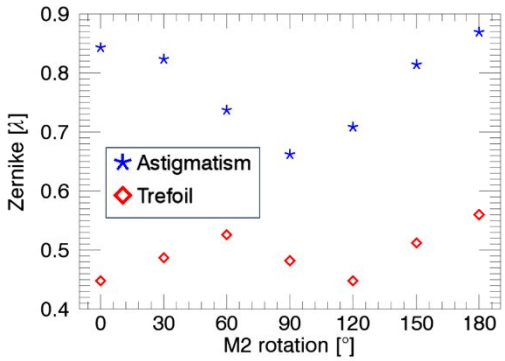

Figure 9. Dependence of astigmatism and trefoil on M2 rotation, with values corrected for temperature. As foreseen, astigmatism shows a minimum every 180°, while trefoil every 120°. To reduce the total PtV, the orientation of M2 minimizing astigmatism was selected.

A typical interferogram and wavefront, taken at T= 23.8°C, after M2 alignment was completed, are presented in Figure 10, left. In Figure 10, right, it is shown also the wavefront after removing tilt, power, coma, astigmatism and spherical aberration, where trefoil is clearly distinguishable.

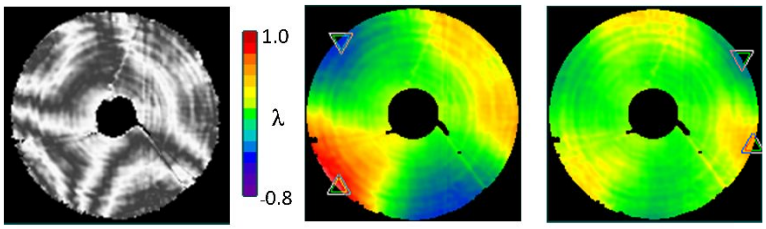

Figure 10. From left to right: a representative interferogram obtained averaging 50 after M2 alignment, with temperature at 23.8°C (we remind the dependence of the Zernike coefficients on temperature); its relative wavefront (PtV is 1.8 λ; rms 0.3 λ) and the wavefront after removing main aberrations, where the trefoil is clearly visible.

The last step of M2 AIV was its gluing, with Hysol 9493 (Figure 11). Even though during the first curing phase (about 2 hours) M2 could still be re-aligned to M1, the operation introduced coma aberration above the requirement (of the order of 0.075 λ) and a variation in the spherical aberration. Furthermore, the minimization of the power is obtained at the temperature corresponding to the moment in which the glue gets sufficiently stiff (about 3 hours after gluing). After glue curing, the manipulator was removed and new wavefronts were taken. The obtained results, dependent on temperature, are shown in Figure 8 right column.
A picture of the telescope taken after completing the tube integration, alignment and verification wrt OBA is shown in Figure 11 right.

Figure 11 *Left*: glue injection to fix M2 to the spider. *Right*: OBA and tube assembled and aligned.

6. CONCLUSIONS

TEL DM alignment, integration and verification of the Tube (M1-M2) have been successfully completed at INAF-Padova laboratories. The main outcomes of this activity are a few lessons-learned, which translated into new strategies elaborated by LEONARDO for PFM, both in the definition of GSEs, in the glue injection and the alignment strategy itself. Furthermore, hands-on experience, along with tip and tricks discovered along the way can certainly help to speed up the alignment process of the PFM, which is supposed to start in a few weeks. Next steps on DM side include BEO optics integration to its mechanics and BEO alignment to the tube. A few TEL DM optical quality verification are also foreseen: an interferometric double-pass test and the measure of the defocused PSF radius (defined as 90% of Encircled Energy) over the entire Field of View.

7. AKNOWLEDGMENTS

CHEOPS activities in Italy are supported by the Italian Space Agency (ASI) - Agreement ASI-INAF n. 2013-016-R.0 09/07/2013.

REFERENCES

[1] Broeg, C., Fortier, A., Ehrenreich, D., Alibert, Y., Baumjohann, W., Benz, W., Deleuil, M., Gillon, M., Ivanov, A., Liseau, R., Meyer, M., Oloffson, G., Pagano, I., Piotto, G., Pollacco, D., Queloz, D., Ragazzoni, R., Renotte, E., Steller, M., Thomas N. and the CHEOPS team, "CHEOPS: A Transit Photometry Mission for ESA's Small Mission", EPJ Web of Conferences 47, 03005 (2013)

[2] Fortier, A., Wehmeier U.J., Benz W., Broeg C., Cessa V., Ehrenreich D., Thomas N., "CHEOPS: a Space Telescope for Ultra-high Precision Photometry of Exoplanet Transits", Proc. SPIE 9143, 91432J (2014)

[3] Rando, N., Asquier, J., Corral Van Damme, C., Isaak, K., Ratti, F., Safa, F., Southworth, R., Broeg, C., Benz, W., "ESA CHEOPS mission: development status", SPIE Proc. This conference (2016)

[4] Beck, T., Fortier,A. Broeg, C., Malvasio, L., Cessa, V., Piazza, D., Benz, W., Thomas, N., Magrin, D., Viotto, V., Bergomi, M, Ragazzoni, R., Pagano, I., Peter, G., Buder, Plesseria, J-Y D., Steller, M., Ottensamer, R., Ehrenreich, D. , Corral, C., Isaak, K., Ratti, F., Rando, N., Ngan, I., "CHEOPS: status summary of the instrument development" SPIE Proc. This conference (2016)

[5] Blecha, L., Zindel, D., Cottard, H., Beck, T., Cessa, V., Broeg, C., Ratti, F., Rando, N. "Analytical optimization and test validation of the submicron dimensional stability of the CHEOPS space telescope's CFRP structure", SPIE Proc. This conference (2016)

[6] Bergomi, M., Viotto, V., Magrin, D., Dima, M., Greggio, D., Farinato, J., Marafatto, L., Ragazzoni, R., Munari, M., Pagano, I., Scandariato, G., Scuderi, S., Beck, T., Buxton, R., Piazza, D., Benz, W., Broeg, C., Cessa, V., Piotto, G., "AIV procedure for a CHEOPS demonstration model", SPIE Proc., 9143, 91435B (2014)

[7] Magrin, D., Farinato, J., Umbriaco, G., Kumar Radhakrishnan Santhakumari, K., Bergomi, M., Dima, M., Greggio, D., Marafatto, L., Ragazzoni, R., Viotto, V., Munari, M., Pagano, I., Scandariato, G., Scuderi, S., Piotto, G.; Beck, T.; Benz, W.; Broeg, C.; Cessa, V.; Fortier, A.; Piazza, D., "Shaping the PSF to nearly top-hat profile: CHEOPS laboratory results", SPIE Proc., 9143, 91434L (2014)